Article

Decarboxylative Phosphine Synthesis: Insights into the Catalytic, Autocatalytic, and Inhibitory Roles of Additives and Intermediates

Shengfei Jin, Graham C. Haug, Vu T. Nguyen, Carsten Flores-Hansen, Hadi D. Arman, and Oleg V. Larionov

ACS Catal., **Just Accepted Manuscript** • DOI: 10.1021/acscatal.9b03366 • Publication Date (Web): 23 Sep 2019

Decarboxylative Phosphine Synthesis: Insights into the Catalytic, Autocatalytic, and Inhibitory Roles of Additives and Intermediates

Shengfei Jin, Graham C. Haug, Vu T. Nguyen, Carsten Flores-Hansen, Hadi D. Arman, and Oleg V. Larionov*

Department of Chemistry, The University of Texas at San Antonio, San Antonio, Texas 78249, United States

Supporting Information Placeholder

ABSTRACT: Phosphines are among the most widely used ligands, catalysts, and reagents. Current synthetic approaches to phosphines are dominated by nucleophilic displacement reactions with organometallic reagents. Here, we report a radical-based approach to phosphines that proceeds by a cross-electrophile coupling of chlorophosphines and redox-active esters. The reaction allows for the synthesis of a broad range of substituted phosphines that were not readily attainable with present methods. Our experimental and DFT computational studies also clarified the catalytic, autocatalytic, and inhibitory roles of additives and intermediates, as well as the mechanistic details of the photocatalytic and zinc-mediated redox modes that can have implications for mechanistic interpretation of other cross-electrophile coupling reactions.

KEYWORDS autocatalysis, biphosphine, carboxylic acid, phosphine, photocatalysis, redox-active ester, zinc activation

1. INTRODUCTION

The impact of phosphines on chemistry is broad, spanning organic, inorganic, organometallic, and analytical chemistry, materials science, and biochemistry.[1] Fine-tuning of steric and electronic properties of phosphines enabled a wide range of new transition metal-catalyzed carbon−carbon and carbon−heteroatom bond-forming reactions that revolutionized organic synthesis.[2] Phosphines have also emerged as efficient organocatalysts[3] and reagents,[4] further enhancing their impact on synthetic methodology. Most of synthetic methods used to access phosphines rely on reactions of air-sensitive organometallic reagents or phosphide salts that suffer from limited scope, tedious purification, and low yields.[5] In contrast, radical phosphine synthesis remains less explored and is not used in synthetic applications, despite the reduced steric hindrance and enhanced reactivity of carbon- and phosphorus-centered radical intermediates, as well as structural diversity of radical precursors that can enable access to phosphines with previously unattainable substitution patterns.[6] The limitations of the available radical phosphine methods include narrow substrate scope, use of toxic organotin reagents, and the oxidative isolation conditions or use of pentavalent phosphorus precursors that require a separate reduction step for readjustment of the phosphorus atom oxidation state.

Importantly, while some progress has been achieved in the functionalization of alkenes by radical phosphination and related additions,[7] other types of carbon−phosphorus(III) bond forming transformations, in particular, radical cross-electrophile coupling reactions[8] have remained relatively unexplored. However, recent examples of reactions of organohalides by Yorimitsu and Oshima, as well as Studer and Smith point to the significant potential of this approach.[9]

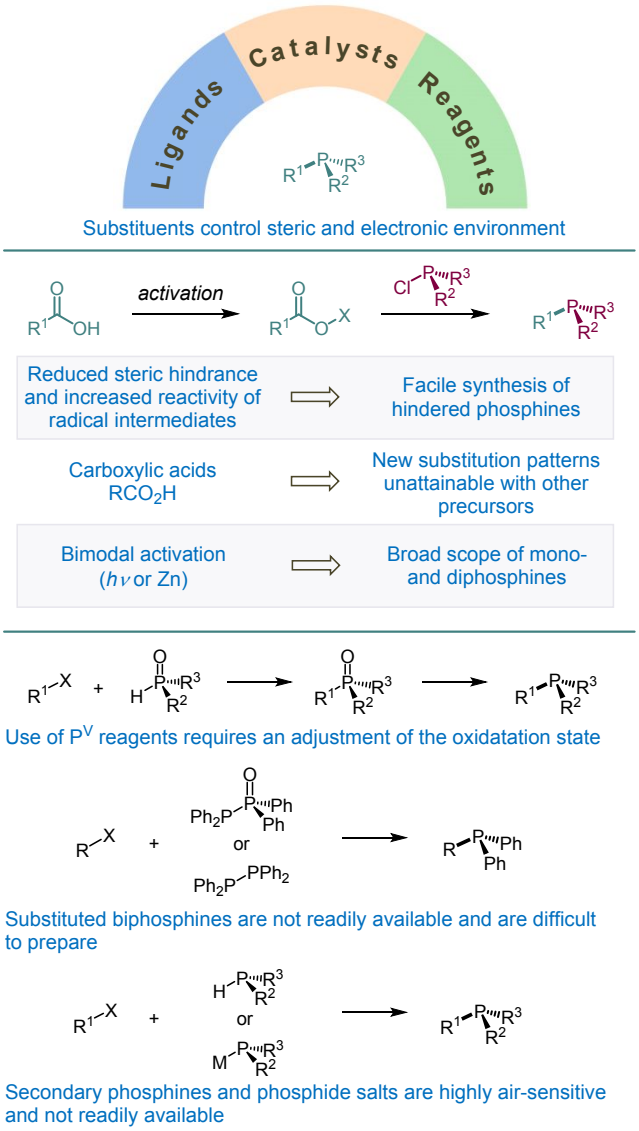

Figure 1. Decarboxylative Phosphine Synthesis from Carboxylic Acids

Since the scope of typical precursors to phosphines is limited to alkyl and aryl halides and organometallic reagents derived from them, use of carboxylic acids as radical precursors for the

phosphine synthesis can greatly expand the structural diversity of phosphines. Carboxylic acids are abundant among natural products and industrial commodity chemicals. They can serve as sources of carbon-centered radicals, and a number of efficient carbon–carbon and carbon–heteroatom bond-forming reactions were recently developed, in particular with redox-active esters.[10] Interestingly, redox-active esters can participate in cross-coupling reactions with other electrophiles, but few mechanistic details of these synthetically powerful transformations are known. Several recent studies highlighted the complex interplay of effects of the reducing metal,[11] additives and catalysts, but mechanistic understanding remains limited. We, therefore, considered the reaction of redox-active esters with chlorophosphines that are common organophosphorus reagents (Figure 1). Chlorophosphines are readily synthetically accessible and are more air-stable than secondary phosphines (R_2PH) or phosphide salts (R_2PM). In addition, the use of chlorophosphines will obviate the oxidation state adjustment step that would be necessary for pentavalent phosphorus reagents. Prior attempts to use redox-active esters to create carbon−phosphorus(III) bonds required highly toxic and pyrophoric white phosphorus or phosphorus-sulfur reagents and did not result in production of phosphines.[12] Thus, the decarboxylative phosphine synthesis from carboxylic acids has remained elusive.

Herein, we describe a broad-scope phosphine synthesis from carboxylic acids and chlorophosphines that can operate bimodally under thermal catalyst-free and photocatalytic conditions. The reaction provides simple access to a wide range of phosphines. We also provide mechanistic details that highlight the importance of additive and autocatalytic effects on the redox processes underlying this and other cross-electrophile coupling reactions.

2. RESULTS AND DICUSSION

Synthetic studies. Initial studies showed that, under the optimal conditions, phosphine **1** was produced in 82% yield in a reaction of chlorophosphine **2** with *N*-hydroxyphthalimide (NHPI) ester **3** in the presence of 30 mol% triamine PMDTA in DMF after 3 h, and in 98% after 12 h, resulting in the 95% isolated yield (Table 1). The reaction was substantially less efficient without PMDTA. Other amines (e.g., TMEDA and DIPEA) or Fe and Ni salts did not significantly improve the efficiency of the phosphine synthesis. Although, a beneficial effect of Lewis acid additives, e.g., lithium salts, was previously demonstrated in some cross-electrophile couplings of redox-active esters,[11] they did not improve the yield of the phosphine synthesis (e.g., entry 7). Finally, DMF was found to be the optimal solvent, while *N*-hydroxyphthalimide ester **3** was superior to other redox-active *N*-alkoxy reagents (e.g., **4** and **5**).

We further proceeded with the study of the scope of the phosphine synthesis. The reaction was tested with a variety of NHPI esters of carboxylic acids **6** (Table 2). Primary carboxylic acids were converted to phosphines **7-12** in good yields. Air-sensitive phosphines were isolated as borane complexes after treatment with borane solution in tetrahydrofuran. Phosphine-borane complexes are air-stable compounds that can be readily isolated by column chromatography and used directly as phosphine ligand precursors for cross-coupling reactions.[13] The reaction afforded glutamic and aspartic acid-derived phosphines **10** and **11**. The decarboxylative phosphine synthesis can also be used to access bisphosphines, as shown for the new dppp-type phosphine **12**. Secondary carboxylic acids also produced corresponding phosphines **13-22** bearing acyclic and cyclic alkyl groups in good yields. Phosphines **18-20** were produced stereoselectively as *trans*-isomers. Notably, the reaction enables facile access to sterically-hindered phosphine **22** in the free form and as a borane complex **21** with the sterically-demanding tetramethylcyclopropyl group. A tartaric acid-derived phosphine **20** can also be prepared in good yield. Phosphine-borane complexes can be readily converted to free phosphines on treatment with DABCO (e.g., **21** to

Table 1. Reaction Conditions for the Decarboxylative Phosphine Synthesis from Carboxylic Acids.[a]

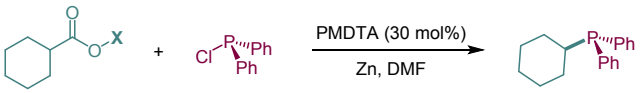

3-5 2 1

Entry	Deviation from standard conditions	Yield, %
1	No change	82, (98,[b] 95[c])
2	No PMDTA	55
3	DIPEA instead of PMDTA	70
4	TMEDA instead of PMDTA	63
5	$Fe(acac)_3$ (5 mol%) instead of PMDTA	60
6	$Ni(dtbbpy)Br_2$ (5 mol%) instead of PMDTA	58
7	LiCl (0.5 equiv.) instead of PMDTA	53
8	MeCN instead of DMF	34
9	Ester **4** instead of **3**	30
10	Ester **5** instead of **3**	0

[a] Reaction conditions: chlorophosphine **2** (0.4 mmol), ester **3** (0.6 mmol, 1.5 equiv.), PMDTA (30 mol%), Zn (1.2 mmol, 3.0 equiv.), DMF (0.4 mL), r.t., 3 h. Yields were determined by ^{1}H NMR spectroscopy with 1,4-dimethoxybenzene as an internal standard. [b] After 12 h. [c] Isolated yield. PMDTA: *N,N,N′,N″,N″*-pentamethyldiethylenetriamine, DIPEA: diisopropylethylamine, TMEDA: *N,N,N′,N′*-tetramethylethylenediamine.

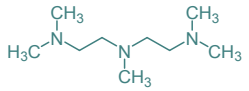
PMDTA

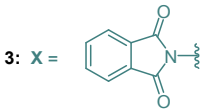

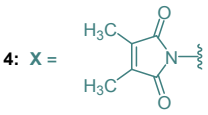

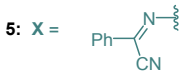

22 in 95% yield) and to the corresponding phosphonium tetrafluoroborate salts (e.g., **21** to **22·HBF$_4$** in 91% yield) that can also be used as air-stable phosphine precursors for transition metal-catalyzed cross-coupling reactions.[14]

Tertiary alkyl phosphines are key ligands for many cross-coupling reactions.[2] We were delighted to see that phosphines **23-31** bearing a variety of tertiary alkyl groups can be readily prepared from the corresponding carboxylic acids by the decarboxylative phosphine synthesis. Tertiary alkyl groups with rings of various sizes were installed, allowing for facile adjustment of steric and electronic environment around the phosphorus atom. The structures of phosphine borane complexes **18**, **25** and **27** were confirmed by X-ray crystallography. Additionally, the structure of phosphine **22** was confirmed after conversion to the corresponding *trans*-Pd(**22**)$_2$Cl$_2$ complex. The phosphine syntheses can be set up outside of a glovebox (e.g., **1**, **7** and **21**) and carried out on gram scales (e.g., **22** and **27**). Carboxylic acids can also be converted to the corresponding NHPI esters in situ and directly subjected to the decarboxylative phosphine synthesis (e.g., phosphines **7-9**, and **21**).

The scope of the reaction was further studied with substituted chlorophosphines (Table 3). The reaction proceeded in good

yields with chlorophosphines bearing both electron-withdrawing and electron-donating substituents in the aryl ring in the meta and para positions (**32-36**). Heteroaryl substituents in chlorophosphines, e.g., 2-furyl, can also be tolerated (**37**).

Table 2. Scope of the Decarboxylative Phosphine Synthesis from Carboxylic Acids and NHPI Esters.[a]

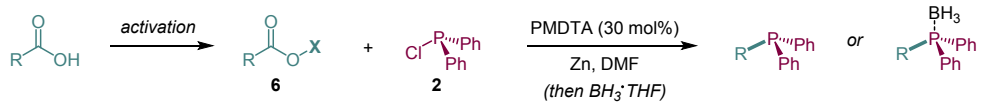

Primary

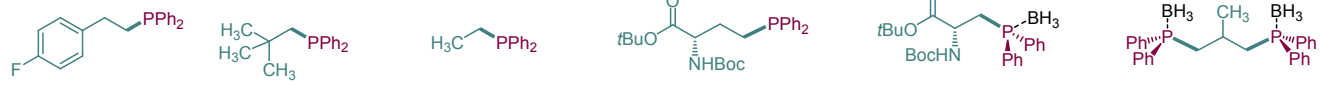

7, 96% (82%,[b] 90%[c]) **8**, 92% (70%[b]) **9**, 97% (75%[b]) **10**, 56% **11**, 66% **12**, 53%[d]

Secondary

13, 96% **1**, 95% (89%[c]) **14**, 75% **15**, 66% **16**, 78% **17**, 95%

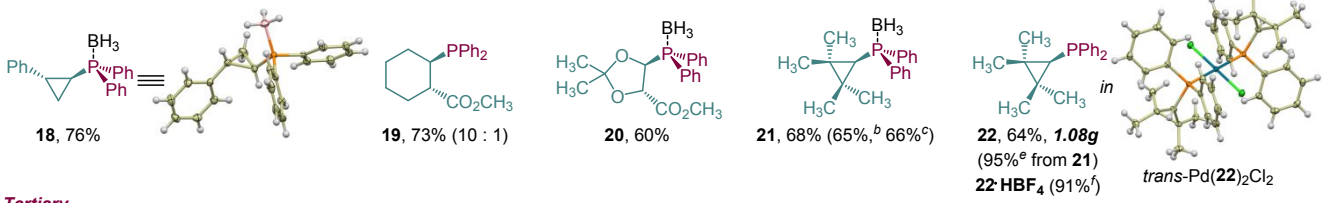

18, 76% **19**, 73% (10 : 1) **20**, 60% **21**, 68% (65%,[b] 66%[c]) **22**, 64%, ***1.08g*** (95%[e] from **21**) **22**·HBF_4 (91%[f]) *in* *trans*-Pd(**22**)$_2$$Cl_2$

Tertiary

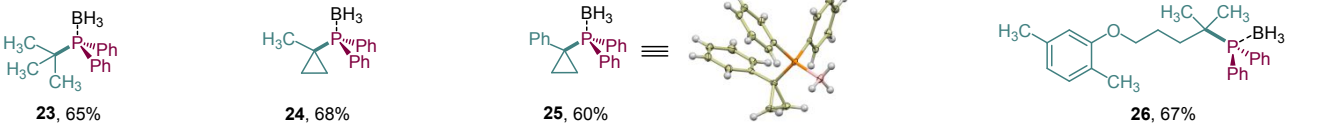

23, 65% **24**, 68% **25**, 60% **26**, 67%

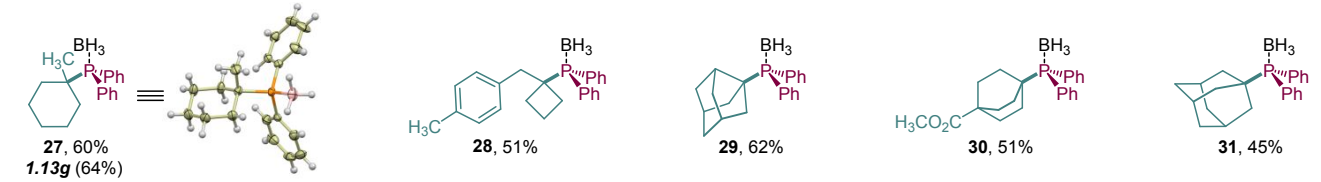

27, 60% ***1.13g*** (64%) **28**, 51% **29**, 62% **30**, 51% **31**, 45%

[a] *N*-Hydroxyphthalimide esters **6** were used. Reaction conditions for small scale experiments: chlorophosphine **2** (0.4 mmol), ester **6** (0.6−0.8 mmol, 1.5−2.0 equiv.), PMDTA (30 mol%), Zn (1.2 mmol, 3.0 equiv.), DMF (0.25−0.4 mL), r.t., 12 h. [b] Yield with ester **6** prepared in situ from carboxylic acid, *N*-hydroxyphthalimide (1.5 equiv.), and diisopropylcarbodiimide (1.5 equiv.). [c] Reaction was set up outside of a glovebox. [d] Chlorophosphine **2** (3 equiv.) and Zn (6 equiv.) were used. [e] Reaction conditions: DABCO, THF, 80 °C, 3 h. [f] Reaction conditions: HBF_4, DCM, rt, 1 h.

Alkyl-substituted chlorophosphines were also suitable coupling partners (e.g., **38** and **39**). Further studies showed that diversely substituted chlorophosphines can be readily coupled with a variety of esters **6** bearing primary, secondary and tertiary alkyl groups (**40-52**). Interestingly, the reaction can also be extended to dichlorophosphines via a twofold coupling with redox-active esters, resulting in formation of two C−P bonds, as shown for phosphine-borane product **53**.

The decarboxylative phosphine synthesis method enables access to phosphines with functional groups that are incompatible with synthetic methods based on organometallic reagents (e.g., phosphines **10**, **11**, **19** and **20**). Furthermore, the availability of diversely substituted cyclic and acyclic carboxylic acids provides an easy entry to phosphines with previously unexplored structural and electronic environments that would not be readily accessible with currently used methods (e.g., **21**, **25**, **29**, and **30**). Several of the tertiary alkyl substituents (e.g., 2,2,3,3,-tetramethylcyclopropyl, tecyl) that are readily introduced with the present method can provide enhanced steric environment that is distinct from the commonly used *tert*-butyl group (See additional discussion in the SI).

Given the recent progress in the development of photocatalytic methods, we were also interested in translating the zinc-mediated decarboxylative phosphine synthesis into a photocatalytic process. Indeed, after initial optimization studies, we observed formation of a variety of phosphines from chlorophosphines and esters **6** in the presence of DIPEA and 0.5−1 mol% $[Ir(ppy)_2bpy]PF_6$ under either LED irradiation (λ_{max} = 400 nm) or sunlight. Phosphines bearing a variety of alkyl groups were easily accessed, including bisphosphines **54-57** with variable alkylidene chain length, as well as diverse substituents on the phosphorus atoms and variedsteric environment (Table 4). In particular, bisphosphines **55** and **57** feature the sterically-demanding structural elements that may be difficult to introduce by other methods and that may significantly alter catalytic behavior of corresponding metal complexes. The photocatalytic variant of the decarboxylative phosphine synthesis tolerated chlorophosphines bearing alkyl and aryl substituents that could be successfully coupled with primary, secondary, and tertiary carboxylic acids (**13**, **14**, **22**, **23**, **37**, **46**,

48, **52**). The yields were comparable or slightly higher than for the zinc-mediated synthesis with equally broad scope of chlorophosphines and esters **6**.

Table 3. Scope of Chlorophosphines for the Decarboxylative Phosphine Synthesis from Carboxylic Acids and NHPI Esters.[a]

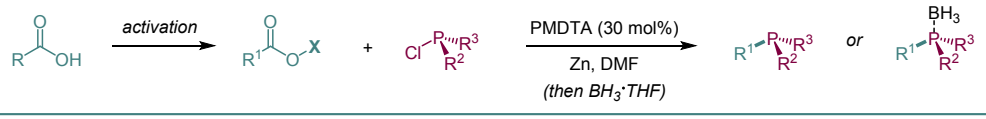

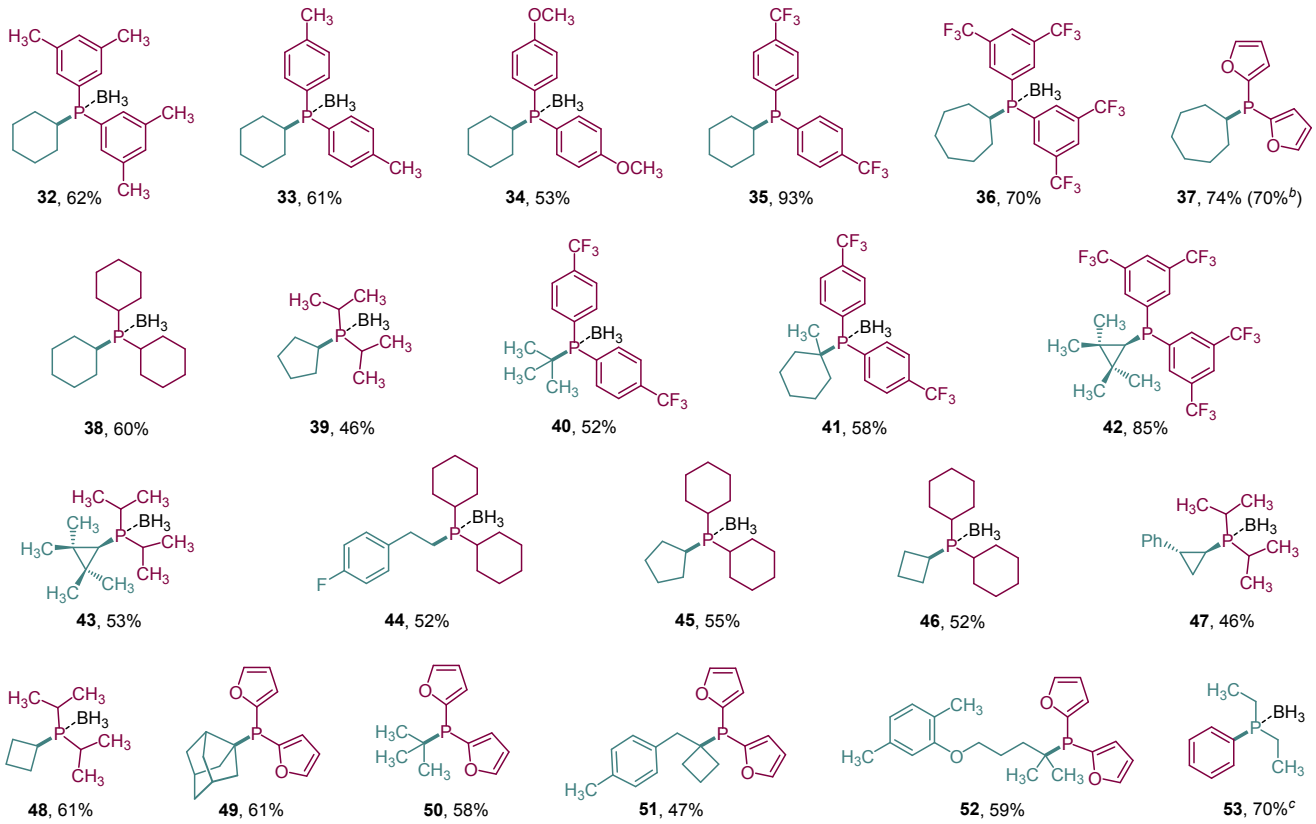

[a] *N*-Hydroxyphthalimide esters **6** were used. Reaction conditions: chlorophosphine (0.4 mmol), ester **6** (0.6–0.8 mmol, 1.5–2.0 equiv.), PMDTA (30 mol%), Zn (1.2 mmol, 3.0 equiv.), DMF (0.25–0.4 mL), r.t., 12 h. [b] Yield with ester **6** prepared in situ from carboxylic acid (1.5 equiv.), *N*-hydroxyphthalimide (1.5 equiv.), and diisopropylcarbodiimide (1.5 equiv.). [c] Ester **6** (4 equiv.) and Zn (6 equiv.) were used.

Mechanistic studies. Given the growing importance of cross-electrophile coupling reactions, we were interested in elucidating the mechanism of the new decarboxylative phosphine synthesis. We were particularly interested in the several notable features of the reaction, including the role of PMDTA and the apparent lack of activation by Lewis acids that are typically required for reactions of esters **6**. Given the known propensity of chlorophosphines to undergo reduction to phosphide salts in the presence of reducing metals, we first explored the pathway that involves formation of zinc phosphides (Ph_2PZnX or $(Ph_2P)_2Zn$) that can then engage esters **6** in an electron transfer process, by analogy to the previously reported reactions of phosphide salts with haloarenes[15] (Figure 2). The tertiary phosphine can then be formed by a recombination of alkyl and diphenylphosphinyl radicals (e.g., by an in-cage recombination[16]), or via an electron-catalyzed process,[17] involving anion radical $RPPh_2^{-\cdot}$[18] (Figure 2).

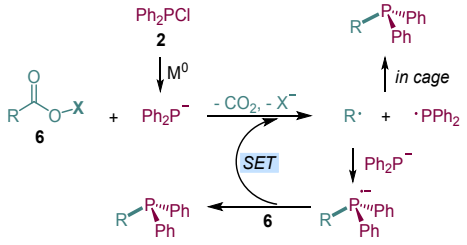

Figure 2. Inoperative phosphide-mediated pathway for the decarboxylative phosphine synthesis from esters 6

However, we found that reactions of ester **3** with zinc phosphide species (Ph_2PZnX or $(Ph_2P)_2Zn$) obtained by a reaction of alkali metal phosphides with zinc halides in various ratios did not produce phosphine **1** under a variety of conditions, including thermal and photochemical activation modes. Similarly, phosphine **1** was not formed when diphenylphosphine (Ph_2PH) was reacted with ester **3** in the presence of bases of varied strength. These results indicate that the aforementioned electron transfer processes are unlikely to be operative under the conditions of the decarboxylative phosphine synthesis. We also ruled out formation of alkylzinc intermediates from the NHPI esters by a two-fold sequential SET reduction of the NHPI esters in experiments with electrophilic reagents (D_2O and benzaldehyde, Figure S1).[19] Thus, the phosphine synthesis from NHPI esters does not involve a reaction of organozinc intermediates with chlorophosphines. On the other hand, involvement of the NHPI ester-derived alkyl radicals was confirmed by radical trapping experiments with 1,1-diphenylethene (Figure S2). In line with this observation and prior reports on the reactivity of HNPI esters,[11a] the products of the reductive decarboxylation of esters **6** in the absence of chlorophosphine **2** were the corresponding alkene and alkane (Figure S3). In order to further clarify the mechanism, we then studied the kinetic profile of the reaction of ester **3** with

chlorophosphine **2** in the absence and in the presence of 30 mol% PMDTA (Figure 3a,b). Remarkably, we observed a rapid disappearance of chlorophosphine **2** that was accompanied by the formation of tetraphenylbiphosphine (**58**). In addition, tetraphenylbiphosphine monoxide (**59**) was also formed as a minor intermediate in the

Table 4. Photocatalytic Decarboxylative Phosphine Synthesis.[a]

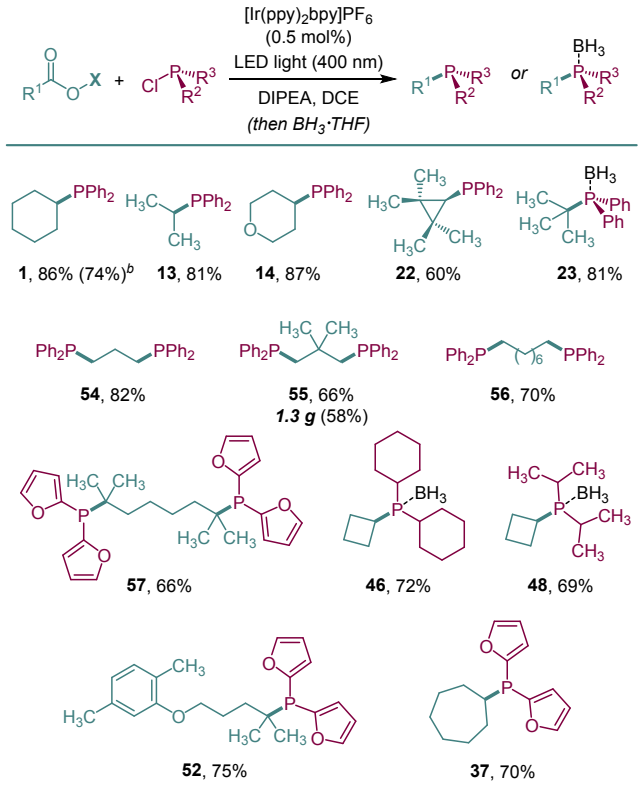

[a] *N*-Hydroxyphthalimide esters **6** were used. Reaction conditions: ester **6** (0.1−0.2 mmol), chlorophosphine (0.3−0.4 mmol, 1.5−4.0 equiv.), $[Ir(ppy)_2bpy]PF_6$ (0.5−1 mol%), DIPEA (4−6 equiv.), DCE (2 mL), LED light (λ_{max} = 400 nm), 22 °C, 8 h. [b] Sunlight-driven experiment.

presence of PMDTA. An induction period was also observed for the formation of phosphine product **1** that roughly corresponded to the accumulation period for biphosphine intermediates **58** and **59**. Further formation of phosphine **1** was accompanied by the proportionate consumption of intermediates **58** and **59**, wherein oxide **59** was more persistent than biphosphine **58** in the presence of PMTDA. Taken together, these results indicate that chlorophosphine **2** is not involved in the reaction with the alkyl radical, directly or via a phosphide salt, but is first converted to biphosphines **58** and **59** that are the actual phosphinating reagents.

Biphosphine **58** is produced in a reaction of chlorophosphine **2** with Zn metal, while monoxide **59** is formed by the base-mediated hydrolysis of chlorophosphine **2** with adventitious water to diphenylphosphine oxide ($Ph_2P(O)H$) that subsequently reacts with chlorophosphine **2** (Figure S4).[20]

We further proceeded with the study of the effect of PMDTA on the reaction performance. Although the reaction proceeded without PMDTA, the yield was lower, even after prolonged stirring (Table 1, entry 2). Furthermore, since esters **6** may undergo reduction with Zn metal, we studied the influence of PMDTA on the reduction process (Figure 3.c). Indeed, the concentration of ester **3** declined over time in the absence of PMDTA. Interestingly, instead of accelerating the reduction of ester **3**, PMDTA attenuated it substantially, suggesting an inhibitory role for PMDTA.

Given the Lewis acidity of the Zn^{II} salts that are formed in the reduction of ester **3** and chlorophosphine **2**, we envisioned that complexation of ester **3** with Zn^{II} could lead to a more thermodynamically favorable reduction process. Increasing concentration of Zn^{II} as the reaction progressed would then lead to an autocatalytic reduction process. Indeed, addition of zinc chloride led to a substantially accelerated reduction of ester **3** (Figure 3.a), confirming the catalytic role of Zn^{II}. Zinc chloride and zinc triflate exhibited similar catalytic behavior, with the triflate being more active, indicating that the catalytic effect is produced by Zn^{II} and not chloride (Figure S5). This result was also supported by DFT computational studies of the one-electron reduction of ester of type **6** in several coordination modes with zinc chloride at the PBE0-D3/Def2-TZVP/SMD level of theory (Figure S6). Furthermore, the sigmoidal shape of the kinetic curves points to the autocatalytic process.[21] Similar autocatalytic effects were previously observed for the Grignard reagent formation (GRF) process, wherein metal salts (e.g., MgX_2) were implicated as key autocatalytic intermediates in the on-surface ion and electron transfer processes, facilitating pitting and desorption.[22] These on-surface effects likely also play a key role in the observed autoamplification of the reduction of ester **3**, in addition to Zn^{II}-mediated activation of ester **3**. Furthermore, a substantial exotherm was observed for the reaction in the presence of zinc chloride that was nearly absent for the $ZnCl_2$-free reaction (Figure S7). The exothermicity of the reaction in the presence of zinc chloride may further contribute to the accelerated decay of ester **3**. Reduction of ester **3** produces the alkyl radical that is one of the central intermediates in the reaction. However, excessively fast reduction may lead to rapid unproductive depletion of ester **3**. PMDTA has been used as a ligand for the stabilization of lower-order zinc complexes, being more effective than mono- and diamines.[23] Thus, one of the roles that PMDTA can play in the decarboxylative phosphine synthesis is dampening the reduction of NHPI esters **6** without completely shutting it down by partially sequestering the Lewis

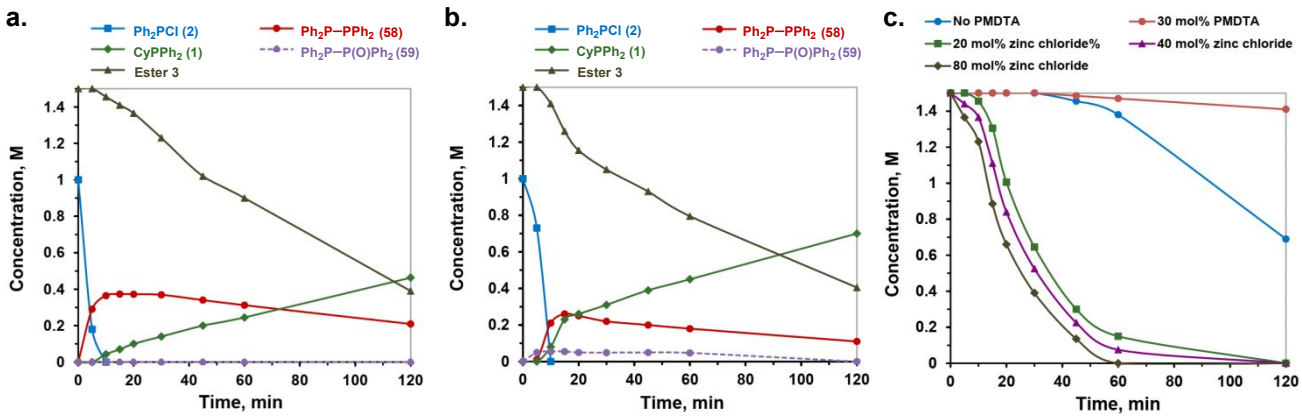

Figure 3. Kinetic studies of the Zn-mediated reaction of ester **3** with chlorophosphine **2**. **a.** Kinetic profile of the Zn-mediated reaction of ester **3** with chlorophosphine **2** in the absence of PMDTA. **b.** Kinetic profile the Zn-mediated reaction of ester **3** with chlorophosphine **2** with 30 mol% PMDTA. **c.** Influence of PMDTA and $ZnCl_2$ on the stability of ester **3** in the presence of Zn (2 equiv.) in DMF.

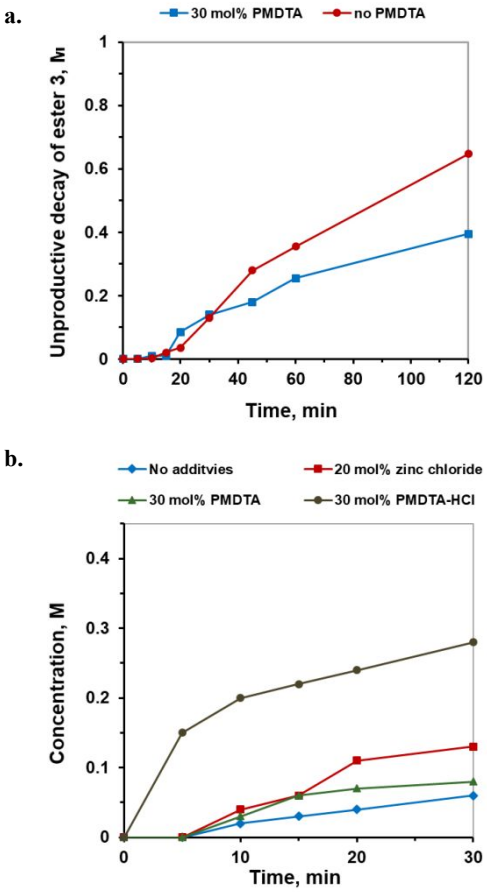

Figure 4. a. Influence of PMDTA on the unproductive decay of ester **3** derived by subtraction of the concentrations of phosphine **1** and ester **3** from the initial concentration of ester **3** (c_0 = 1.5M). **b.** Influence of additives ($ZnCl_2$, PMDTA and PMDTA·HCl) on the production of phosphine **1** in the reaction of ester **3** with biphosphine **58** and Zn (3 equiv.) in DMF.

acidic Zn^{2+} on the metal surface and bringing the reduction rate into alignment with the downstream steps en route to the phosphine product. This protective role of PMDTA is evident in the time course graphs for the concentration of ester **3** in the Zn-mediated reaction with chlorophosphine **2** (Figure 3.a,b) and in the time course graph of the unproductive decay of ester **3** (Figure 4.a). While a rapid consumption of ester **3** is observed in the initial phase (20−40 min) both with and without PMDTA, the consumption did not lead to significant production of phosphine **1** in the reaction without PMDTA, in contrast to the reaction with PMDTA. The unproductive decay also remained consistently lower with PMDTA. A distinctive feature of the kinetic profile of the reaction in the presence of PMDTA is the rapid accumulation of phosphine **1** following an initial induction period (Figure 3.b). The reaction in the absence of PMDTA did not show the same rapid accumulation phase that appears to be to a significant extent responsible for the improved yield of phosphine **1** in the PMDTA-mediated reaction. Since the accumulation phase occurs close to completion of the chlorophosphine reduction phase, we suspected that it may be caused by the increase in the reaction temperature due to the rapid and exothermic chlorophosphine reduction. Indeed, the reaction temperature rapidly rose to 42 °C in the first 12 min for the PMDTA-mediated reaction, coinciding with the phosphine product accumulation phase (Figure S8). However, the exothermic phase was also observed for the reaction in the absence of PMDTA, but without the rapid onset of the phosphine production, indicating that the exotherm is not responsible for the PMDTA effect. This conclusion is also supported by the observation that the PMDTA-mediated reaction exhibited nearly identical kinetic behavior under thermostated and under standard conditions (Figure S9). The exotherm occurred more rapidly in the absence of PMDTA, in line with the observed earlier completion of the chlorophosphine reduction step. In both cases, the exotherm was caused by the reaction of chlorophosphine **2** with zinc, as evidenced by the nearly identical exotherm graphs for the reactions performed in the absence and in the presence of ester **3** (cf. Figures S8 and S10). By analogy with the GRF reaction and the zinc-mediated reduction of ester **3**, the zinc-mediated chlorophosphine reduction can also be autocatalyzed by Zn^{II} salts. Indeed, kinetic experiments with zinc-mediated chlorophosphine reduction demonstrated significant acceleration in the presence of 20 and 40 mol% of zinc chloride (Figure S11). The influence of main group metal salts on the reactivity of zinc with electrophiles remains poorly understood, despite the synthetic importance of organozinc reagents and cross-electrophile couplings. Recent pioneering studies by Blum and co-workers[24] shed light on the role of lithium halides in the acceleration of the reaction of zinc with organohalides. Their studies demonstrated that the salts accelerate the reaction by assisting in the solubilization of organozinc products from the surface of zinc powder. However, lithium chloride was not effective in improving the yield of the phosphine synthesis (Table 1). Furthermore, monitoring of the reaction progress indicated that, although LiCl accelerated production of phosphine **1** in the early stages, it also caused a substantial unproductive decay of ester **3** leading to an overall lower yield of phosphine **1** (Figure S12). These results show that the autocatalytic effect of Zn^{II} salts and other Lewis acids has to be attenuated to align the rates of the upstream alkyl radical production with the downstream steps in the phosphine synthesis.

In order to further clarify the role of PMDTA in the early stages of the reaction and to better understand the dynamics of the decarboxylative phosphine synthesis after completion of the chlorophosphine reduction phase, the reaction was carried out with biphosphine **58** instead of chlorophosphine **2**. As expected, accumulation of phosphine **1** was slow in the absence of PMDTA (Figure 4.b). Addition of PMDTA did not significantly improve the yield (e.g., 8% yield of phosphine **1** with PMDTA and 6% without PMDTA). This result indicates that PMDTA alone does not substantially promote the reaction. In contrast to the reactions with chlorophosphine **2**, the biphosphine **58**-mediated reactions were not accompanied by an exotherm (Figure S13), in line with the observation that the exotherm is caused by the reduction of chlorophosphine. On the other hand, addition of zinc chloride (20 mol%) led to a more significant acceleration, confirming the catalytic role of Zn^{II}.

Amine hydrochloride salts are formed as byproducts of the reaction that produces biphosphine monoxide **59** from chlorophosphine **1** in the presence of an amine and moisture. Both DMF and PMDTA are hygroscopic compounds, and complete exclusion of moisture would be impracticable. Based on the amount of biphosphine monoxide **59** produced in the phosphine synthesis with PMDTA (Figures 3.b and S2), 8−10 mol% PMDTA·HCl is expected to be produced in the reaction mixture. Given the recently suggested role of tertiary amine hydrochloride salts in the activation of zinc powder,[25,] we also studied the influence of PMDTA·HCl on the reaction with biphosphine **58**. Interestingly, a substantial acceleration was observed, indicative

of the important role of PMDTA·HCl in the acceleration of the reaction. Use of freshly distilled DMF and PMDTA to mitigate the influence of adventitious moisture substantially reduced production of biphosphine monoxide **59** and phosphine **1** (Figure S14), further supporting the role of PMDTA·HCl in the observed acceleration.[26]

Collectively, the present study highlights the reinforcing and balancing roles of the autocatalytic effects of zinc activators (Zn^{II}

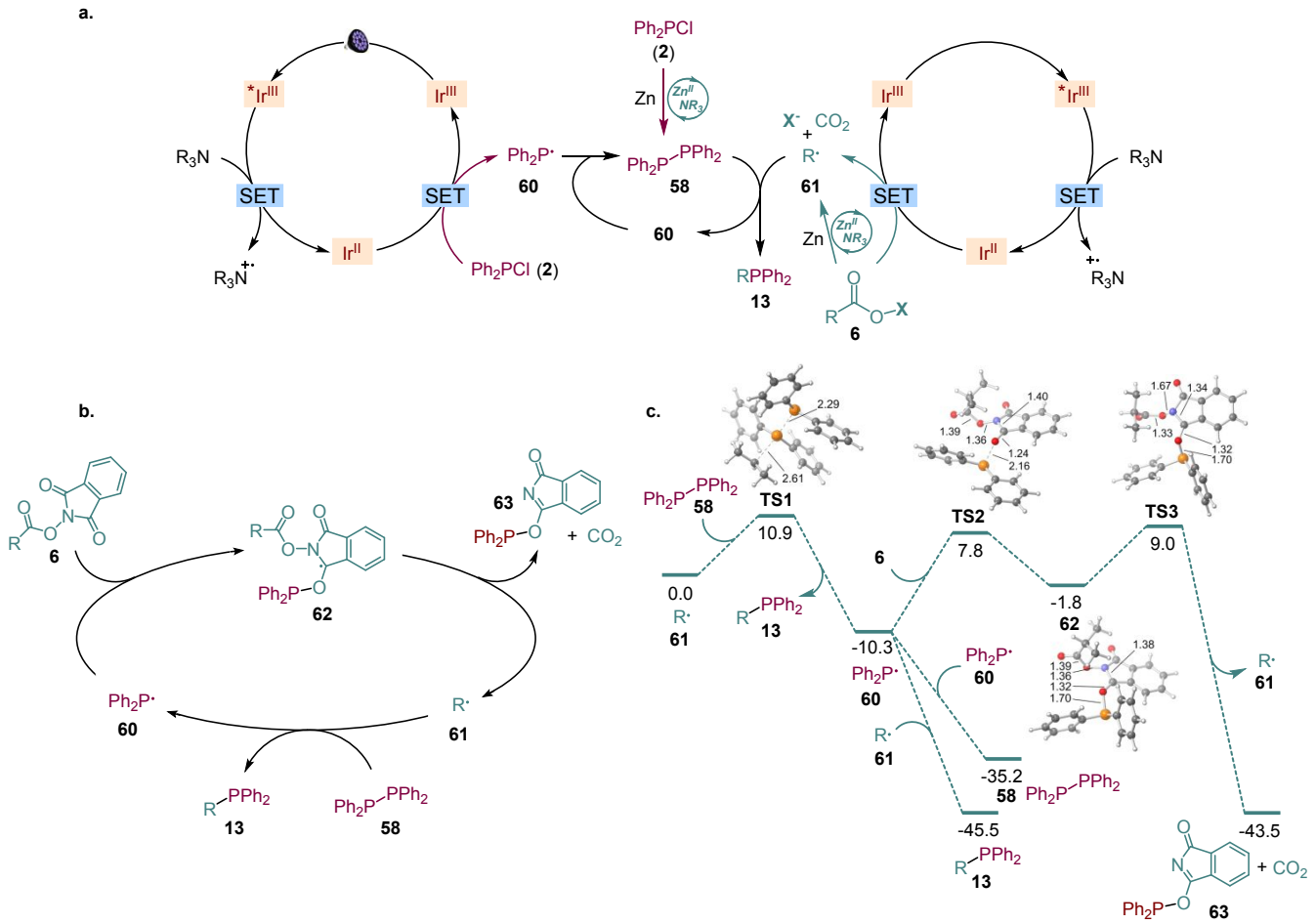

Figure 5. a. Unified mechanistic manifold for the decarboxylative phosphine synthesis from esters **6** and chlorophosphines. **b.** Decarboxylative pathway proceeding via ketyl type intermediate **62**. **c.** DFT computational studies of the homolytic substitution pathway with ester **6** at the PBE0-D3/Def2-TZVP/SMD level of theory, R = isopropyl, Gibbs free energies in kcal/mol.

and amine hydrochloride salts) and the stabilizing effect of amine, coupled with the beneficial role of moisture in the mechanistically complex setting of a cross-electrophile coupling reaction.

The experimental data also show that biphosphine monoxide **59** that is formed in the early stages of the reaction is consumed within the first 2 h of the reaction (Figure 3.c). Biphosphine monoxide **59** can also participate in the homolytic substitution reaction with the alkyl radical, as was previously demonstrated by Kawaguchi and Ogawa.[7b] The radical substitution takes place at the P^{III} terminus, producing the corresponding phosphine.[7b]

From a synthetic perspective, although both biphosphine **58** and monoxide **59** can be used as reagents for homolytic phosphination, they and their substituted congeners are not readily available and are too air-sensitive for synthetic applications. The use of more readily available and stable chlorophosphines as reagents for homolytic carbon−phosphorus(III) bond formation in conjunction with the decarboxylative approach to organic radicals allows for by-passing of synthetically tedious phosphination and phosphinylation procedures, while providing access to structurally novel phosphines without the necessity to readjust the phosphorus oxidation state. Current limitations of the method include the lack of reactivity of redox esters of aromatic carboxylic acids, as well as the inability of the method to effect the triple C−P bond formation from phosphorus trichloride.

We further proceeded with the mechanistic study of the photocatalytic decarboxylative phosphine synthesis. The excited state of the photocatalyst is not sufficiently reducing ($E^0_{red}(Ir^{III}/*Ir^{II})$ = −0.85 V (SCE))[27,28] to effect the reduction of chlorophosphine **2** (E^0_{red} = −1.38 V (SCE))[29] and esters **6** (E^0_{red} = −1.28 to −1.37 V (SCE)).[30] Instead, reductive quenching of the photocatalyst by DIPEA produces the thermodynamically competent reductant (E^0_{red} = −1.42 V (SCE) for Ir^{III}/Ir^{II}) that is capable of reducing both reactants (i.e., **2** and **6**). Indeed, emission quenching was observed for the photocatalyst in the presence of DIPEA (see Figures S15−S20 and additional discussion in the SI). Furthermore, both ester **3** and chlorophosphine **2** underwent photocatalytic reduction in the presence of DIPEA (see Figures S21). In the case of the NHPI esters, the major products were the corresponding alkene and alkane in line with the expected reactivity of the intermediate alkyl radical (Figure S3). On the other hand, chlorophosphine **2** underwent photocatalyzed reduction to biphosphine **58**, and the intermediacy of diphenylphosphinyl radical ($Ph_2P^{\cdot}$, **60**) was confirmed by EPR studies with α-phenyl-*N*-*tert*-butylnitrone (NBP) as a spin-trap reagent (Figure S22). Given that self-terminations of non-persistent radicals proceed at diffusion-controlled rates in the absence of other competing pathways,[31] the self-termination of phosphinyl radical **60** is expected to lead to rapid accumulation of the dimer, biphosphine **58**, in line with the experimental

observations. Further, biphosphine **58** was confirmed to be a competent phosphinating reagent en route to phosphine **1** and an intermediate in the photocatalytic decarboxylative phosphine synthesis (Figures S23 and S24) under the photocatalytic conditions. Taken together, these results indicate that the photocatalytic reaction and the zinc-mediated synthesis provide alternative portals to the same mechanistic manifold (Figure 5.a). The two reaction modes differ in the timing of the chlorophosphine reduction and homolytic substitution steps. While the chlorophosphine reduction phase is fast and largely precedes the decarboxylative phosphination in the Zn-mediated reaction, the two phases show greater temporal overlap in the photocatalytic mode.

Given the propensity of related silyl, germyl and stannyl radicals to add to carbonyl groups at the oxygen atom, resulting in ketyl radicals,[32] we also investigated the reaction of phosphinyl radical **60** with ester **6** as a competing pathway that enables regeneration of alkyl radical **61** (Figure 5.b). If this pathway were operative, it would have significant implications for the overall mechanism, since it would entail a radical chain process. According to this mechanism, addition of phosphinyl radical **60** to ester **6** would produce intermediate **62** that further undergoes N−O bond homolysis and decarboxylation, giving rise to alkyl radical **61** and *O*-phosphinyl phthalimide derivative **63**. Product **63** can serve as an experimental marker for the involvement of the pathway. Interestingly, formation of *O*-phosphinyl phthalimide derivative **63** was not observed experimentally for the zinc-mediated and photocatalytic conditions, suggesting that the reaction of phosphinyl radical **60** is not operative in the decarboxylative phosphine synthesis. Additional experiments were performed to further evaluate the mechanism. Ester **3** was reacted with diphenylphosphine (Ph_2PH) in the presence of radical initiators that are known to produce phosphinyl radical **60** (Figure S25). In all cases, no phosphine product was formed and only biphosphine **58** was observed, indicating that self-termination of phosphinyl radical **60** outcompetes the reaction of radical **60** with the NHPI ester.

DFT computational studies (PBE0-D3/Def2-TZVP/SMD, several other functionals and basis sets were also used and gave comparable results, see SI) were then carried out to investigate further details of the reaction mechanism and to clarify these experimental observations (Figure 5.c). The reaction of radical **61** (R = isopropyl) with biphosphine **58** was found to be exergonic by 10.3 kcal/mol, proceeding with a barrier of 10.9 kcal/mol. The resulting phosphinyl radical **60** undergoes barrierless dimerization, regenerating biphosphine **58**, as described above, in an exergonic step (−24.9 kcal/mol). Cross-termination of radicals **60** and **61** was also found to proceed exergonically (−35.2 kcal/mol) and without a barrier. Significantly, the reaction of phosphinyl radical **60** with ester **6** proceeds endergonically (8.5 kcal/mol) and with a comparatively high barrier of 18.1 kcal/mol to give ketyl-type intermediate **62**. Subsequent breakup of intermediate **62**, on the other hand, is exergonic (−41.7 kcal/mol) with a barrier of 10.8 kcal/mol. Thus, the computational studies show that the very fast formation of biphosphine **58** from phosphinyl radical **60** outcompetes the comparatively slow and thermodynamically unfavorable ketyl **62** formation step, resulting in suppression of the ketyl radical **62**-based mechanism.

CONCLUSION

In conclusion, this paper describes a simple and scalable method of decarboxylative phosphine synthesis. The reaction produces a variety of phosphines in good to excellent yields under mild conditions in zinc-mediated and photocatalytic modes. The mechanism of the reaction and the competition dynamics of autocatalytic and inhibitory effects, as well as involvement of alternative pathways were investigated experimentally and computationally to produce a unified mechanistic perspective that can be useful in the mechanistic analysis of other cross-electrophile couplings and carbon−phosphorus bond-forming reactions.

AUTHOR INFORMATION

Corresponding Author

oleg.larionov@utsa.edu

Notes

The authors declare no competing financial interest.

ACKNOWLEDGMENT

Financial support by the Welch Foundation (AX-1788), the NSF (CHE-1455061 and CHE-1625963), and ACS PRF is gratefully acknowledged. The authors acknowledge the Texas Advanced Computing Center (TACC) at the University of Texas at Austin for providing computational resources.

ASSOCIATED CONTENT

Supporting Information

Experimental, spectral, and X-ray crystallographic details for all new compounds and all reactions reported. This material is available free of charge via the Internet at http://pubs.acs.org.

REFERENCES

(1) (a) Iaroshenko, V., Ed.; *Organophosphorus Chemistry: From Molecules to Applications*; Wiley-VCH: Weinheim, Germany, 2019. (b) Corbridge, D.E.C. *Phosphorus: Chemistry, Biochemistry and Technology*, 6th ed.; CRC Press: Boca Raton, Florida, 2013. (c) Priegert, A. M.; Rawe, B. W.; Serin, S. C.; Gates, D. P. Polymers and the P-Block Elements. *Chem. Soc. Rev.* **2016**, *45*, 922−953.

(2) (a) Martin, R.; Buchwald, S. L. Palladium-Catalyzed Suzuki-Miyaura Cross-Coupling Reactions Employing Dialkylbiaryl Phosphine Ligands. *Acc. Chem. Res.* **2008**, *41*, 1461–1473. (b) Hartwig, J. F. *Organotransition Metal Chemistry, from Bonding to Catalysis*; University Science Books: New York, 2010. (c) Kamer, P.C.J.; van Leeuwen, P. W. N. M., Eds.; *Phosphorus(III) ligands in homogeneous catalysis; design and synthesis*; John Wiley & Sons: Hoboken, New Jersey, 2012.

(3) (a) Methot, J. L.; Roush, W. R. Nucleophilic Phosphine Organocatalysis. *Adv. Synth Catal.* **2004**, *346*, 1035−1050. (b) Guo, H.; Fan, Y. C.; Sun, Z.; Wu, Y.; Kwon, O. Phosphine Organocatalysis. *Chem. Rev.* **2018**, *118*, 10049−10293.

(4) Murphy, P. J. *Organophosphorus Reagents: A Practical Approach in Chemistry*; Oxford University Press: Oxford, UK, 2004.

(5) (a) Allen, D. W.; Loakes, D.; Tebby, J. C., Eds; *Organophosphorus Chemistry*; The Royal Society of Chemistry: Cambridge, UK, 2012. (b) Wauters, I.; Debrouwer, W.; Stevens, C. V. Preparation of Phosphines Through C–P Bond Formation. *Beilstein J. Org. Chem.* **2014,** *10,* 1064–1096.

(6) (a) Leca, D.; Fensterbank, L.; Lacote, E.; Malacria, M. Recent Advances in the Use of Phosphorus-Centered Radicals in Organic Chemistry. *Chem. Soc. Rev.* **2005**, *34*, 858−865. (b) Van der Jeught, S.; Stevens, C. V. Direct Phosphonylation of Aromatic Azaheterocycles. *Chem. Rev.* **2009**, *109*, 2672−2702. (c) Yorimitsu, H. Homolytic Substitution at Phosphorus for C–P Bond Formation in Organic Synthesis. *Beilstein J. Org. Chem.* **2013**, *9*, 1269−1277.

(7) (a) Lamas, M. C.; Studer, A. Radical Alkylphosphanylation of Olefins with Stannylated or Silylated Phosphanes and Alkyl Iodides. *Org. Lett.* **2011**, *13*, 2236−2239. (b) Sato, Y.; Kawaguchi, S.-i.; Nomoto, A.; Ogawa, A. Highly Selective Phosphinylphosphination of Alkenes with Tetraphenyldiphosphine Monoxide. *Angew. Chem., Int. Ed.* **2016**, *55*, 9700−9703. (c) Okugawa, Y.; Hirano, K.; Miura, M. Copper-Catalyzed Vicinal Diphosphination of Styrenes: Access to 1,2-Bis(diphenylphosphino)ethane-Type Bidentate Ligands from Olefins. *Angew. Chem. Int. Ed.* **2016**, *55*, 13558–13561. (d) Otomura, N.; Okugawa, Y.; Hirano, K.; Miura, M. *vic*-Diphosphination of Alkenes with Silylphosphine under Visible Light-Promoted Photoredox Catalysis. *Org. Lett.* **2017**, *19*, 4802−4805. (e) Otomura, N.; Hirano, K.; Miura, M. Diphosphination of 1,3-Dienes with Diphosphines under Visible Light-

Promoted Photoredox Catalysis. *Org. Lett.* **2018**, *20*, 7965−7968. For recent examples of phophonylation with P^V reagents, see: (f) Zhang, P.-Z.; Zhang, L.; Li, J.-A.; Shoberu, A.; Zou, J.-P.; Zhang, W. Phosphinoyl Radical Initiated Vicinal Cyanophosphinoylation of Alkenes. *Org. Lett.* **2017**, *19*, 5537−5540. (g) Sato, Y.; Nishimura, M.; Kawaguchi, S.-i.; Nomoto, A.; Ogawa, A. Reductive Rearrangement of Tetraphenyldiphosphine Disulfide To Trigger the Bisthiophosphinylation of Alkenes and Alkynes. *Chem. Eur. J.* **2019**, *25*, 6797–6806. (h) Buquoi, J. Q.; Lear, J. M.; Gu, X.; Nagib, D. A. Heteroarene Phosphinylalkylation via a Catalytic, Polarity-Reversing Radical Cascade. *ACS Catal.* **2019**, *9*, 5330−5335.

(8) (a) Everson, D. A.; Weix, D. J. Cross-Electrophile Coupling: Principles of Reactivity and Selectivity. *J. Org. Chem.* **2014**, *79*, 4793–4798. (b) Lucas, E. L.; Jarvo, E. R. Stereospecific and Stereoconvergent Cross-Couplings Between Alkyl Electrophiles. *Nat. Rev. Chem.* **2017**, *1*, 0065. (c) Cherney, A. H.; Kadunce, N. T.; Reisman, S. E. Catalytic Asymmetric Reductive Acyl Cross-Coupling: Synthesis of Enantioenriched Acyclic α,α-Disubstituted Ketones. *J. Am. Chem. Soc.* **2013**, *135*, 7442−7445. (d) Moragas, T.; Correa, A.; Martin, R. Metal-Catalyzed Reductive Coupling Reactions of Organic Halides with Carbonyl-Type Compounds. *Chem. Eur. J.* **2014**, *20*, 8242−8258.

(9) (a) Sato, A.; Yorimitsu, A.; Oshima, K. Radical Phosphination of Organic Halides and Alkyl Imidazole-1-carbothioates. *J. Am. Chem. Soc.* **2006,** *128,* 4240–4241. (b) Vaillard, S. E.; Muck-Lichtenfeld, C.; Grimme, S.; Studer, A. Homolytic Substitution at Phosphorus for the Synthesis of Alkyl and Aryl Phosphanes. *Angew. Chem., Int. Ed.* **2007**, *46*, 6533−6536. (c) Bruch, A.; Ambrosius, A.; Fröhlich, R.; Studer, A.; Guthrie, D.; Zhang, B. H.; Curran, D. P. Memory of Axial Chirality in Aryl Radical Phosphanylations. *J. Am. Chem. Soc.* **2010**, *132*, 11452–11454. (d) Bruch, A.; Fukazawa, A.; Yamaguchi, E.; Yamaguchi, S.; Studer, A. Bis(phosphoryl)-Bridged Biphenyls by Radical Phosphanylation: Synthesis and Photophysical and Electrochemical Properties. *Angew. Chem., Int. Ed.* **2011**, *50*, 12094–12098. (e) Zhou, W.; MacLeod, K. C.; Smith, K. M. Controlling Secondary Alkyl Radicals: Ligand Effects in Chromium Catalyzed C−P Bond Formation. *Organometallics* **2012**, *31*, 7324−7327. (f) Kawaguchi, S.-i.; Minamida, Y.; Ohe, T.; Nomoto, A.; Sonoda, M.; Ogawa, A. Synthesis and Properties of Perfluoroalkyl Phosphine Ligands: Photoinduced Reaction of Diphosphines with Perfluoroalkyl Iodides. *Angew. Chem., Int. Ed.* **2013**, *52*, 1748–1752.

(10) (a) Okada, K.; Okamoto, K.; Oda, M. A New and Practical Method of Decarboxylation: Photosensitized Decarboxylation of *N*-Acyloxyphthalimides via Electron-Transfer Mechanism. *J. Am. Chem. Soc.* **1988**, *110*, 8736−8738. (b) Okada, K.; Okamoto, K.; Morita, N.; Okubo, K.; Oda, M. Photosensitized Decarboxylative Michael Addition Through *N*-(Acyloxy)phthalimides via an Electron-Transfer Mechanism. *J. Am. Chem. Soc.* **1991**, *113*, 9401−9402. (c) Allen, L. J.; Cabrera, P. J.; Lee, M.; Sanford, M. S. *N*-Acyloxyphthalimides as Nitrogen Radical Precursors in the Visible Light Photocatalyzed Room Temperature C–H Amination of Arenes and Heteroarenes. *J. Am. Chem. Soc.* **2014**, *136*, 5607–5610. (d) Xuan, J.; Zhang, Z.-G.; Xiao, W.-J. Visible-Light-Induced Decarboxylative Functionalization of Carboxylic Acids and Their Derivatives. *Angew. Chem. Int. Ed.* **2015**, *54*, 15632–15641. (e) Griffin, J. D.; Zeller, M. A.; Nicewicz, D. A. Hydrodecarboxylation of Carboxylic and Malonic Acid Derivatives via Organic Photoredox Catalysis: Substrate Scope and Mechanistic Insight. *J. Am. Chem. Soc.* **2015**, *137*, 11340–11348. (f) Shaw, M. H.; Twilton, J.; MacMillan, D. W. C. Photoredox Catalysis in Organic Chemistry. *J. Org. Chem.* **2016**, *81*, 6898–6926. (g) Jamison, C. R.; Overman, L. E. Fragment Coupling with Tertiary Radicals Generated by Visible-Light Photocatalysis. *Acc. Chem. Res.* **2016**, *49*, 1578−1586. (h) Cornella, J.; Edwards, J. T.; Qin, T.; Kawamura, S.; Wang, J. Pan, C-M.; Gianatassio, R.; Schmidt, M. A.; Eastgate, M. D.; Baran, P. S. Practical Ni-Catalyzed Aryl-Alkyl Cross-Coupling of Secondary Redox-Active Esters, *J. Am. Chem. Soc.* **2016**, *138*, 2174−2177. (i) Qin, T.; Cornella, J.; Li, C.; Malins, L.R.; Edwards, J. T.; Kawamura, S.; Maxwell, B. D.; Eastgate, M. D.; Baran, P. S. A General Alkyl-Alkyl Cross-Coupling Enabled by Redox-Active Esters and Alkylzinc Reagents, *Science* **2016**, *352*, 801−805. (j) Huihui, K. M. M.; Caputo, J. A.; Melchor, Z.; Olivares, A. M.; Spiewak, A. M.; Johnson, K. A.; DiBenedetto, T. A.; Kim, S.; Ackerman, L. K. G.; Weix, D. J. Decarboxylative Cross-Electrophile Coupling of *N*-Hydroxyphthalimide Esters with Aryl Iodides. *J. Am. Chem. Soc.* **2016**, *138*, 5016−5019. (k) Xue, W.; Oestreich, M. Copper-Catalyzed Decarboxylative Radical Silylation of Redox-Active Aliphatic Carboxylic Acid Derivatives. *Angew. Chem., Int. Ed.* **2017**, *56*, 11649–11652. (l) Wang, D.; Zhu, N.; Chen, P.; Lin, Z.; Liu, G. Enantioselective Decarboxylative Cyanation Employing Cooperative Photoredox Catalysis and Copper Catalysis. *J. Am. Chem. Soc.* **2017**, *139*, 15632–15635. (m) Zhao, W.; Wurz, R. P.; Peters, J. C.; Fu, G. C. Photoinduced, Copper-Catalyzed Decarboxylative C–N Coupling to Generate Protected Amines: an Alternative to the Curtius Rearrangement. *J. Am. Chem. Soc.* **2017**, *139*, 12153–12156. (n) Schwarz, J.; König, B. Decarboxylative Reactions with and without Light – A Comparison. *Green Chem.* **2018**, *20*, 323−361. (o) Tlahuext-Aca, A.; Candish, L.; Garza-Sanchez, R. A.; Glorius, F. Decarboxylative Olefination of Activated Aliphatic Acids Enabled by Dual Organophotoredox/Copper Catalysis. *ACS Catal.* **2018**, *8*, 1715–1719. (p) Proctor, R.S.; Davis, H. J.; Phipps, R. J. Catalytic Enantioselective Minisci-Type Addition to Heteroarenes. *Science* **2018**, *360*, 419–422. (q) Mao, R.; Balon, J.; Hu, X. Cross-Coupling of Alkyl Redox-Active Esters with Benzophenone Imines: Tandem Photoredox and Copper Catalysis. *Angew. Chem., Int. Ed.* **2018**, *130*, 9645–9648. (r) Ishii, T.; Kakeno, Y.; Nagao, K.; Ohmiya, H. *N*-Heterocyclic Carbene-Catalyzed Decarboxylative Alkylation of Aldehydes. *J. Am. Chem. Soc.* **2019**, *141*, 3854−3858. (s) Wang, J.; Cary, B. P.; Beyer, P. D.; Gellman, S. H.; Weix, D. J. Ketones from Nickel-Catalyzed Decarboxylative, Non-Symmetric Cross-Electrophile Coupling of Carboxylic Acid Esters. *Angew. Chem., Int. Ed.* **2019**, *58*, 12081−12085.

(11) (a) Ni, S.; Padial, N. M.; Kingston, C.; Vantourout, J. C.; Schmitt, D. C.; Edwards, J. T.; Kruszyk, M.; Merchant, R. R.; Mykhailiuk, P. K.; Sanchez, B.; Yang, S.; Perry, M.; Gallego, G. M.; Mousseau, J. J.; Collins, M. R.; Cherney, R. J.; Lebed, P. S.; Chen, J. S.; Qin, T.; Baran, P. S. A Radical Approach to Anionic Chemistry: Synthesis of Ketones, Alcohols, and Amines. *J. Am. Chem. Soc.* **2019**, *141*, 6726−6739. (b) Wang, J.; Lundberg, H.; Asai, S.; Martín-Acosta, P.; Chen, J. S.; Brown, S.; Farrell, W.; Dushin, R.; O'Donnell, C. J.; Ratnayake, A. S.; Richardson, P.; Liu, Z.; Qin, T.; Blackmond, D. G.; Baran, P. S. Kinetically Guided Radical-Based Synthesis of $C(sp^3)$−$C(sp^3)$ Linkages on DNA. *Proc. Natl. Acad. Sci. U.S.A.* **2018**, *115*, E6404.

(12) (a) Barton, D. H. R.; Bridon, D.; Zard, S.Z. Radical Decarboxylative Phosphorylation of Carboxylic Acids. *Tetrahedron Lett.* **1986,** *27,* 4309–4312. (b) Barton, D. H. R.; Zhu, J. Elemental White Phosphorus as a Radical Trap: A New and General Route to Phosphonic Acids. *J. Am. Chem. Soc.* **1993**, *115,* 2071–2072.

(13) (a) Darcel, C.; Kaloun, E. B.; Merdès, R.; Moulin, D.; Riegel, N.; Thorimbert, S.; Genêt, J.P.; Jugé, S. Direct Use of Chiral or Achiral Organophosphorus Boranes as Pro-Ligands for Transition Metal Catalyzed Reactions. *J. Organomet. Chem.* **2001**, *624*, 333–343. (b) Brisset, H.; Gourdel, Y.; Pellon, P.; LeCorre, M. Phosphine-Borane Complexes; Direct Use in Asymmetric Catalysis. *Tetrahedron Lett.* **1993**, *34*, 4523−4526. (c) Dolhem, F.; Johansson, M. J.; Antonsson, T.; Kann, N. *P*-Chirogenic α-Carboxyphosphine Boranes as Effective Pre-Ligands in Palladium-Catalyzed Asymmetric Reactions. *Synlett* **2006**, 3389–3394. (d) Nguyen, D. H.; Bayardon, J.; Salomon-Bertrand, C.; Jugé, S.; Kalck, P.; Daran, J-C.; Coppel, Y.; Urrutigoïty, M.; Gouygou, M. Modular Phosphole-Methano-Bridged-Phosphine(Borane) Ligands. Application to Rhodium-Catalyzed Reactions. *Organometallics* **2012**, *31*, 857−869.

(14) Netherton, M. R.; Fu, G. C. Air-Stable Trialkylphosphonium Salts: Simple, Practical, and Versatile Replacements for Air-Sensitive Trialkylphosphines. Applications in Stoichiometric and Catalytic Processes. *Org. Lett.* **2001**, *3*, 4295– 4298.

(15) (a) Alonso, R. A.; Bardon, A.; Rossi, R. A. Relative Reactivities of Amide, Diphenylphosphide, and Diphenylarsenide Ions toward Aryl Radicals. *J. Org. Chem.* **1984**, *49*, 3584−3587. (b) Russell, G.A.; Khanna, R.K. Electron-Transfer Processes. Part 40. Reaction of Alkyl Radicals with Diphenylphosphide Anion. *Phosphorus Sulfur Relat. Elem.* **1987**, *29*, 271−274. (c) Austin, E.; Alonso, R. A.; Rossi, R. A. Aromatic Radical Nucleophilic Substitution Reactions Initiated by Sodium Amalgam in Liquid Ammonia. *J. Org. Chem.* **1991**, *56*, 4486.

(16) Lorand, J. P. The Cage Effect. *Prog. Inorg. Chem.* **1972**, *17*, 207−325.

(17) Studer, A.; Curran, D. P. Catalysis of Radical Reactions: a Radical Chemistry Perspective. *Angew. Chem., Int. Ed.* **2016**, *55*, 58–102.

(18) (a) Kaim, W.; Hanel, P.; Bock, H. Radical-Anions. 53. The Reduction of Triphenylphosphane Derivatives to Their Radical-Anions and to the Radical Dianion of Dibenzophosphole. *Z. Naturforsch., B: J. Chem. Sci.* **1982**, *37*, 1382−1387. (b) Kaim, W.; Lechnerknoblauch, U.; Hanel, P.; Bock, H. Organophosphorus Redox Systems. *J. Org. Chem.* **1983**, *48*, 4206−4209.

(19) Involvement of elctron transfer processes and the intermediacy of alkyl radicals in the formation of organozinc reagents from alkyl halides and zinc was proposed by Rieke: Guijarro, A.; Rosenberg, D. M.; Rieke, R. D. The Reaction of Active Zinc with Organic Bromides. *J. Am. Chem.*

Soc. **1999**, *121*, 4155−4167.

(20) McKechnie, J.; Payne, D. S.; Sim, W. Tetraphenyldiphosphine Monoxide. *J. Chem. Soc.* **1965**, 3500−3501.

(21) Moore J. W.; Pearson R.G. *Kinetics and Mechanism*, 3rd Ed.; John Wiley & Sons: Hoboken, New Jersey, 1981; p. 26.

(22) Shao, Y.; Liu, Z.; Huang, P.; Liu, B. A Unified Model of Grignard Reagent Formation. *Phys. Chem. Chem. Phys.* **2018**, *20*, 11100−11108.

(23) (a) Pafford, R. J.; Rauchfuss, T. B. Effect of Ancillary Ligands on the Reactivity and Structure of Zinc Polysulfido Complexes. *Inorg. Chem.* **1998**, *37*, 1974−1980. (b) Nurchi, V. M.; Crisponi, G.; Sanna, G.; Pérez-Toro, I.; Niclos-Gutierrez, J.; Gonzalez-Perez, M. J.; Domínguez Martín, A. Complex Formation Equilibria of Polyamine Ligands with Copper(II) and Zinc(II). *J. Inorg. Biochem.* **2019**, *194*, 26−33.

(24) (a) Feng, C.; Cunningham, D. W.; Easter, Q. T.; Blum, S. A. Role of LiCl in Generating Soluble Organozinc Reagents. *J. Am. Chem. Soc.* **2016**, *138*, 11156−11159. (b) Feng, C.; Easter, Q. T.; Blum, S. A. Structure−Reactivity Studies, Characterization, and Transformation of Intermediates by Lithium Chloride in the Direct Insertion of Alkyl and Aryl Iodides to Metallic Zinc Powder. *Organometallics* **2017**, *36*, 2389−2396. (c) Jess, K.; Kitagawa, K.; Tagawa, T. K. S.; Blum, S. A. Microscopy Reveals: Impact of Lithium Salts on Elementary Steps Predicts Organozinc Reagent Synthesis and Structure. *J. Am. Chem. Soc.* **2019**, *141*, 9879−9884. For a recent example of the use of LiCl as an activator in a cross-electrophile coupling, see: Huang, L.; Ackerman, L.K.G.; Kang, K.; Parsons, A. M.; Weix, D. J. LiCl-Accelerated Multimetallic Cross-Coupling of Aryl Chlorides with Aryl Triflates. *J. Am. Chem. Soc.* **2019**, *141*, 10978−10983.

(25) Ye, K.-Y.; McCallum, T.; Lin, S. Bimetallic Radical Redox-Relay Catalysis for the Isomerization of Epoxides to Allylic Alcohols. *J. Am. Chem. Soc.* **2019**, *141*, 9548−9554.

(26) PMDTA·HCl may facilitate clearance of zinc phthalimide from the zinc surface and additionally accelerate on-surface electron transfer processes.

(27) All E^0 values are reported for solutions in acetonitrile that is also a suitable solvent for the photocatalytic decarboxylative phosphine synthesis (e.g., phosphine **1** was produced in 75% yield).

(28) Goldsmith, J. I.; Hudson, W. R.; Lowry, M. S.; Anderson, T. H.; Bernhard, S. Discovery and High-Throughput Screening of Heteroleptic Iridium Complexes for Photoinduced Hydrogen Production. *J. Am. Chem. Soc.* **2005**, *127*, 7502–7510.

(29) (a) Matschiner, H.; Tanneberg, H. Zur Elektrochemischen Reduktion von Chlorphosphanen. *Z. Chem.* **1980**, *20*, 218−219. (b) Hall, T. J.; Hargis, J. H. Electrochemical Reduction of Trivalent Organophosphorus Compounds: Mechanism and Products from Phosphorus−Heteroatom Bond Cleavage. *J. Org. Chem.* **1986**, *51*, 4185−4189.

(30) Lackner, G. L.; Overman, L. E. Constructing Quaternary Carbons from *N* ‐(Acyloxy)phthalimide Precursors of Tertiary Radicals Using Visible-Light Photocatalysis. *J. Org. Chem.* **2015**, *80*, 6025−6036.

(31) (a) Zard, S. Z. *Radical Reactions in Organic Synthesis*; Oxford University Press: Oxford, UK, 2003; pp. 6−13. (b) Nonhebel, D. C.; Walton, J. C. *Free-Radical Chemistry: Structure and Mechanism*; Cambridge University Press: Cambridge, UK, 1974; pp. 205−210.

(32) (a) Barton, D. H. R.; Blundell, P.; Jaszberenyi, J. C. Acyl Derivatives of Hydroxamic Acids as a Source of Carbon Radicals. *Tetrahedron Lett.* **1989**, *30*, 2341−2344. (b) Alberti, A.; Chatgilialoglu, C. Addition of Tris(trimethylsilyl)silyl Radicals to the Carbonyl Group. *Tetrahedron* **1990**, *46*, 3963−3972. (c) Beckwith, A. L. J.; Roberts, D. H. *J. Am. Chem. Soc.* **1986**, *108*, 5893−5901. (d) Bernardoni, S.; Lucarini, M.; Pedulli, G. F.; Valgimigli, L.; Gevorgyan, V.; Chatgilialoglu, C. Addition Reactions of Tris(trimethylsilyl)germyl Radicals to Unsaturated Compounds. An EPR and Product Study. *J. Org. Chem.* **1997**, *62*, 8009–8014. (e) Sugawara, T.; Otter, B. A.; Ueda, T. *Tetrahedron Lett.* **1988**, *29*, 75−78. (f) Hays, D. S.; Fu, G. C. *J. Org. Chem.* **1998**, *63*, 6375−6381. (f) Bebbington, D.; Bentley, J.; Nilsson, P. A.; Parsons, A. F. *Tetrahedron Lett.* **2000**, *41*, 8941−8945.

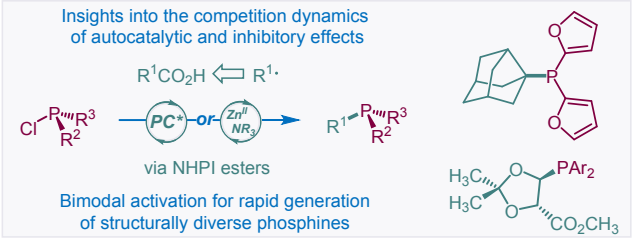

TOC graphic